Non-Fixed Scatterers and Their Effects on MIMO Multicarrier Fading Communication Channels

Hamidreza Saligheh Rad
School of Engineering and Applied Sciences
Harvard University
Cambridge, MA 02138, USA
Email: hamid@seas.harvard.edu

Saeed Gazor
Department of Electrical and Computer Engineering
Queen's University
Kingston, ON, K7M 1B5, Canada
Email: s.gazor@queensu.ca

Pooya Shariatpanahi
Department of Electrical Engineering
Sharif University of Technology
Tehran, Iran
Email: pooyashariat@yahoo.com

***Abstract*—There are two types of scatterers in a multipath propagation environment: fixed and non-fixed scatterers. Fixed scatterers like buildings, mountains and tree stems do not move, while non-fixed (moving) scatterers like cars, people and tree leaves move from their initial positions. In addition to different movements of the mobile station (MS) that cause different kinds of Doppler fading, movements of non-fixed scatterers are also anticipated to generate other kinds of fading/correlation. This fading changes depend on the type of the propagation environment and the type of movements of local surrounding scatterers. In this paper we characterize these effects in terms of temporal correlations. In this study we assume constant speed for the MS and random displacements for scatterers based on stationary-increment Wiener vector process. As it will be verified, these random movements have direct effect on the channel process power spectral density (PSD).**

I. Introduction

Available models to characterize the cross-correlation function (CCF) of multiple-input multiple-output (MIMO) outdoor wireless communication channels mostly assume a constant speed vector for the MS, while they consider immobile scatterers on the azimuth plane[1]. In reality some of these scatterers are fixed, while some others move around in a non-systematic form. Studying the effect of these scatterers' displacements cause new fading(s) and correlations in the CCF of the channel process $h(t,\omega)$. This is especially true for scatterers close to the mobile station (MS).

There are very few works in the literature to consider the effects of local scatterers' displacements on wireless channels, e.g. [1]–[3]. Thoen, Van der Perre and Engels in [1] assume uniform distribution for the angle between the direction of movement and the direction orthogonal to the reflecting surface, uniform distribution for the reflection angle associated to moving scatterer, and uniform distribution $U[0, v_{max})$ for the speed of scatterers, while the propagation environment is assumed to be isotropic. In such a situation, the temporal correlation function is appeared as an averaged form of the square of a zero-order Bessel function [4]. Molisch in [2] proposes a systematic measurement of the moving-scatterer statistics with special orientation to see its effects on MIMO capacity. As the angular power spectrum is an essential parameter for the capacity, shadowing of components coming from a certain direction will have a major impact. Medlbo, Berg, and Harrysson in [3] perform an analysis based on measurements to see the effects of the important finding caused by the movements of scatterers in the vicinity of either MS or BS antenna. This analysis is supported by a simple model, based on a single moving scatterer (a person), which shows good agreement with their measurements.

In this paper we assume a random displacement model for the movements of scatterers based on stationary-increment Wiener processes, while we assume a constant MS speed vector on the azimuth plane. The scattering environment is a two-dimensional (2D) non-isotropic propagation medium when multi-element directional antennas (MEA)s are employed at both receiver and transmitter ends. In this scenario, both stations receive a large number of waveforms reflected from moving scatterers. The effect of random movements of each scatterer changes the relative distance of the scatterer to the MS coordinate. Therefore, it has a direct effect on the propagation delay caused by that scatterer. While the MS moves with a constant speed on the azimuth plane, it may have other movements like arbitrary rotations around the azimuth axis[2], in the situation when the MS moving trajectory path is not a straight line. In this situation, almost all rotational movements of the MS are to align the coordinate with the direction of its trajectory. These rotations are usually very slowly varying with time and with very low impacts on the CCF, therefore we ignore them in this paper [5].

The rest of this paper is organized as follows: Notations and assumptions are introduced in Section II. In Section III, the proposed CCF is derived and analyzed. In Section IV power spectral density analysis is provided along with numerical examples. Finally, conclusions are summarized in Section V.

II. Non-Isotropic Scattering Medium with Non-Fixed (Moving) Scatterer

Figure 1 shows a pair of BS-MS antennas from a MIMO communication system with directional antennas and in a

[1]By definition, the azimuth plane is the two-dimensional horizontal plane.

[2]By definition, the azimuth axis is the axis passing through the MS and perpendicular to the azimuth plane.

1930-529X/07/$25.00 © 2007 IEEE

TABLE I
NOTATIONS AND THEIR DESCRIPTIONS

O^B, O^M	BS coordinate, MS coordinate
$h_{pm}(t,\omega)$	Channel transfer function between pth BS antenna element and mth MS antenna element
$\mathbf{a}_p^B$	Position vector of the pth antenna element on the BS side relative to O^B
$\mathbf{a}_m^M$	Position vector of the mth antenna element on the MS side relative to O^M
$\mathbf{\Theta}_i^B$	The unity vector pointing to the direction-of-departure (DOD) of the ith dominant path from the BS
$\mathbf{\Theta}_i^M$	The unity vector pointing to the direction-of-arrival (DOA) of the ith dominant path to the MS
Θ_i^B; Θ_i^M	DOD of the ith dominant path from the BS; DOA of the ith dominant path to the MS
$G_p^B(\Theta^B;\omega)$	Antenna propagation pattern of the p^{th} antenna element of the BS
$G_m^M(\Theta^M;\omega)$	Antenna propagation pattern of the m^{th} antenna element of the MS
$\mathbf{X}_i^S(t)$	Displacement vector of the ith scatterer between two time instances 0 and t
$\tau_{p,m;i}$	Delay between pth BS antenna element and mth MS antenna element via ith dominant path
$g_{p,m;i}$	Gain between pth BS and mth MS antenna elements via the ith dominant path, approximated by g_i
ζ_i	Normalized variance of the Normal Wiener process used to represent displacements of the ith scatterer
ϕ_i; ω	Phase contribution along the ith dominant path; Carrier frequency
$\overline{\tau}$; σ	Mean and delay spread of the time-delay distribution function τ_i
$\mathbf{v}$; c	MS speed vector; Wave propagation velocity
η; I	Pathloss exponent; Number of total dominant paths

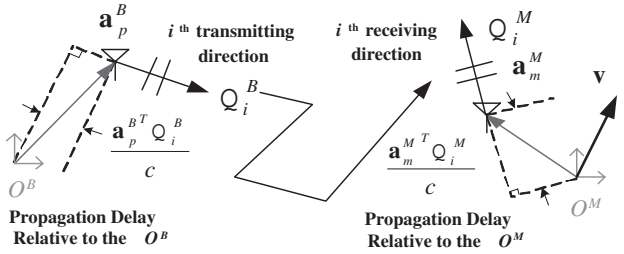

Fig. 1. Moving MS on the azimuth plane with constant speed vector $\mathbf{v}$; pth antenna of the BS located at $\mathbf{a}_p^B$, mth antenna of the MS located at $\mathbf{a}_m^M$ in their local coordinates, and ith propagating path caused by the ith moving scatterer through the scattering medium.

two-dimensional (2D) non-isotropic propagation environment, when scatterers have random displacements and the MS moves with a constant speed vector. As it is well-known, time-variations in a random wireless channel are the direct result of movements of both MS and scatterers. In the set-up of this paper, the initial condition of the MS coordinate O^M is defined with respect to the BS coordinate O^B, while its displacements are characterized by a constant speed vector $\mathbf{v}$. Besides, the displacement vector of the ith scatterer with respect to its initial condition is represented by $\mathbf{X}_i^S(t)$. While these displacements contribute in some delays, initial situations of scatterers produce initial delays which is explained in more details in this section.

Table I presents the employed notations throughout this paper in which superscripts B and M indicate variables at BS and MS sides, respectively. In this paper, we establish the following set-up based on the following assumptions:

A1) We assume that the BS antenna array is immobile in its coordinate O^B, and the MS antenna array moves as a solid object with its coordinate O^M. The displacement of the MS is represented by a 2D constant vector $\mathbf{v}$ to represent linear displacements between O^B and O^M on the azimuth plane and at time t. The displacements of this scatterer, $\mathbf{X}_i^S(t) \triangleq \begin{bmatrix} \mathbf{x}_{i,1}^S(t) \\ \mathbf{x}_{i,2}^S(t) \end{bmatrix}$, follows a 2D stationary-increment Wiener random vector[3] [6, Chapter 10]: The components of $\mathbf{X}_i^S(t)$, $\mathbf{x}_{i,1}^S(t)$ and $\mathbf{x}_{i,2}^S(t)$, are independent non-stationary zero-mean Normal random processes with stationary-independent increments[4]. For the ith scatterer, the properties of $\mathbf{X}_i^S(t)$ and its components are summarized as follows:

a) $\mathbf{x}_{i,1}^S(t)$ and $\mathbf{x}_{i,2}^S(t)$ are independent identically distributed (i.i.d.) zero-mean non-stationary Normal random variables, with variance $\zeta_i t$ ($\zeta_i \geqslant 0$), and autocorrelation $\zeta_i \min(t_1,t_2)$ [6, Chapter 10]:
   - $f_{\mathbf{x}_i^S(t)}(x) = \frac{1}{\sqrt{2\pi\zeta_i t}} e^{-x^2/(2\zeta_i t)}$,
   - $E[\mathbf{x}_i^S(t)] = 0$, and $E[\mathbf{x}_i^{S^2}(t)] = \zeta_i t$,
   - $E[\mathbf{x}_i^S(t_1)\mathbf{x}_i^S(t_2)] = \zeta_i \min(t_1,t_2)$.

b) $\mathbf{x}_{i,1}^S(t)$ and $\mathbf{x}_{i,2}^S(t)$ have independent increments:
   - $E\left[[\mathbf{x}_i^S(t_2) - \mathbf{x}_i^S(t_1)][\mathbf{x}_i^S(t_4) - \mathbf{x}_i^S(t_3)]\right] = 0$ for $t_1 < t_2 < t_3 < t_4$.

c) $\mathbf{x}_{i,1}^S(t)$ and $\mathbf{x}_{i,2}^S(t)$ have stationary-increments:
   - $E\left[\left(\mathbf{x}_i^S(t_2) - \mathbf{x}_i^S(t_1)\right)^2\right] = \zeta_i(t_2 - t_1)$ for $t_1 < t_2$.

Therefore when the ith scatterer moves, it contributes to the delay associated to this propagating path. The

[3]A Wiener process is an independent increment random process which is used to describe a Brownian motion process. A Wiener random vector is a vector whose elements are independent Wiener processes.

[4]**Definition** [7, Chapter 7]: A random process has *independent increments* when the set of n random variables

$$\mathbf{x}(t_1),\ \mathbf{x}(t_2) - \mathbf{x}(t_1), \cdots,\ \mathbf{x}(t_n) - \mathbf{x}(t_{n-1}),$$

are jointly independent for all $t_1 < t_2 < \cdots < t_n$ and for all n.

Definition: A stochastic process $\{\mathbf{x}(t) \mid t \in T\}$ where $T \subset \mathbb{R}$, is said to have stationary increments if the probability distribution function for $\mathbf{x}(s+t) - \mathbf{x}(s)$ is fixed (the same) for all $s \in T$ such that $s + t \in T$. In other words, the distribution for $\mathbf{x}(s+t) - \mathbf{x}(s)$ is a function of "how long" or t, not "when" or s.

A stochastic process that possesses both stationary increments and independent increments is said to have stationary independent increments.

1930-529X/07/$25.00 © 2007 IEEE

analysis of this time-varying delay has been studied in more details in this section.

A2) For the ith propagation path, we associate $\mathbf{\Theta}_i^B$ and $\mathbf{\Theta}_i^M$ as propagation directions, a complex gain caused by the antenna propagation patterns (APP)s $G_p^B(\Theta_i^B;\omega)G_m^M(\Theta_i^M;\omega)$, a time-varying delay $\tau_{p,m;i}(t)$, a path attenuation gain $g_{p,m;i} \approx g_i$, and a path phase shift ϕ_i. The space-time-frequency (STF) channel transfer function (CTF) between the BS antenna at $\mathbf{a}_p^B$ and the MS antenna located at $\mathbf{a}_m^M$ is represented as follows:

$$h_{pm}(t,\omega) \triangleq \sum_{i=1}^{I}\Big\{G_p^B(\Theta_i^B;\omega)G_m^M(\Theta_i^M;\omega) \times g_i\exp\left(j\phi_i - j\omega\tau_{p,m;i}(t)\right)\Big\}. \quad (1)$$

A3) The propagation delay over the ith path is time-varying due to displacements of the ith scatterer from its initial position, as well as movements of the MS, as follows:

$$\tau_{p,m;i}(t) \triangleq \tau_{p,m;i}(0) + \frac{1}{c}\big(\mathbf{X}_i^S(t) + \mathbf{v}t\big)^T\mathbf{\Theta}_i^M, \quad (2)$$

where $(.)^T$ represents the Transpose operation.

A4) At time zero, we decompose the propagation delay of the i^{th} path, $\tau_{p,m;i}(0)$, into three components: one major distance delay and two relative propagation delays with respect to BS and MS local coordinates as follows:

$$\tau_{p,m;i}(0) = \tau_i - \left(\tau_{p;i}^B + \tau_{m;i}^M\right), \quad (3a)$$

$$\tau_{p;i}^B \triangleq \frac{{\mathbf{a}_p^B}^T\mathbf{\Theta}_i^B}{c}, \quad \tau_{m;i}^M \triangleq \frac{{\mathbf{a}_m^M}^T\mathbf{\Theta}_i^M}{c}, \quad (3b)$$

where τ_i represents the distance delay between O^B and O^M, and $\tau_{p;i}^B$ and $\tau_{m;i}^M$ represent relative propagation delays from antenna elements, $\mathbf{a}_p^B$ or $\mathbf{a}_m^M$, to corresponding coordinates, O^B or O^M, respectively [8]. The time-delays τ_i's are assumed to be i.i.d. random variables which are Exponentially distributed. Exponential pdf is a commonly used distribution for the time-delay in outdoor environments [9], [10]. The pdf of the time-delay τ is $f_\tau(x) = \frac{1}{\sigma}e^{-\frac{x-\overline{\tau}+\sigma}{\sigma}}$, $\forall x \geqslant \overline{\tau}-\sigma$, where $\overline{\tau} = E[\tau_i]$ is the mean value used to specify the initial distance between BS and MS coordinates (major propagation distance), and σ is the delay spread. The moment generating function (MGF) of the time-delay is $\mathbf{\Phi}_\tau(s) = E[e^{s\tau}] = \int_{-\infty}^{+\infty} e^{sx}f_\tau(x)dx = \frac{e^{(\overline{\tau}-\sigma)s}}{1-\sigma s}$.

A5) The pdf of the propagation directions, $f^B(\Theta^B)$ and $f^M(\Theta^M)$ over $[-\pi,\pi)$, characterize the non-isotropic propagation environment around the BS and the MS, respectively. Since these pdfs are periodic with period 2π, we can represent them by their FSE pairs as follows:

$$\mathcal{F}_k^B \longleftrightarrow f^B(\Theta^B) \text{ and } \mathcal{F}_k^M \longleftrightarrow f^M(\Theta^M), \quad (4a)$$

$$\mathcal{F}_k = \frac{1}{2\pi}\int_{-\pi}^{\pi} f(\Theta)e^{-jk\Theta}d\Theta \text{ and } f(\Theta) = \sum_{k=-\infty}^{+\infty}\mathcal{F}_k e^{jk\Theta} \quad (4b)$$

Reported measurement results suggest two candidates for these pdfs, namely truncated-Normal and truncated-Laplace distributions (see [11] for more investigations).

A6) The APPs of the pth antenna at the BS and the mth antenna at the MS at frequency ω are taken into account by $G_p^B(\Theta^B;\omega)$ and $G_m^M(\Theta^M;\omega)$, respectively, where $\Theta^B \triangleq \angle\mathbf{\Theta}^B$ and $\Theta^M \triangleq \angle\mathbf{\Theta}^M$ are the propagation directions (DOD or DOA) at the BS and the MS sides, respectively. Complex APPs, $G_p^B(\Theta^B;\omega)$ and $G_m^M(\Theta^M;\omega)$, are periodic functions with the period of 2π. Therefore, we represent them by their FSE pairs (see [11] for the FSE of the APPs of some commonly used antennas):

$$\mathcal{G}_k^B(\omega) \longleftrightarrow G^B(\Theta^B;\omega), \quad (5a)$$
$$\mathcal{G}_k^M(\omega) \longleftrightarrow G^M(\Theta^M;\omega),$$

$$\mathcal{G}_k = \frac{1}{2\pi}\int_{-\pi}^{\pi} G(\Theta)e^{-jk\Theta}d\Theta \text{ and } G(\Theta) = \sum_{k=-\infty}^{+\infty}\mathcal{G}_k e^{jk\Theta} \quad (5b)$$

A7) Assuming that $|\tau_i| \gg \max\left\{|\tau_{p;i}^B|, |\tau_{m;i}^M|\right\}$, the path-gain is given by $g_i = \sqrt{\frac{P}{I}}\ {\tau_i}^{-\frac{\eta}{2}}$, where η is the pathloss exponent and P is a constant. Appropriate values for the pathloss exponent are $\eta = 2$ for free space propagation environments, $\eta = 4$ for rural environments and $\eta = 6$ for crowded urban environments [12].

A8) As a consequence of the planar wave propagation, the path phase shift ϕ_i accurately approximates $\phi_{p,m;i}$. We take into account the phase contribution of scatterers by uncorrelated uniformly distributed random phase changes, i.e. $\phi_i \sim U[-\pi,\pi)$ and $E[\exp(\phi_{i_1} - \phi_{i_2})] = \delta[i_1 - i_2]$, where $\delta[.]$ is the unit impulse.

Substituting (2) in (1), we get:

$$h_{pm}(t,\omega) \triangleq \sum_{i=1}^{I}\Big\{G_p^B(\Theta_i^B;\omega)G_m^M(\Theta_i^M;\omega)g_i \times e^{j\phi_i - j\frac{\omega}{c}\left(\mathbf{X}_i^S(t)+\mathbf{v}t\right)^T\mathbf{\Theta}_i^M - j\omega\tau_{p,m;i}(0)}\Big\}. \quad (6)$$

The frequency shift of the ith received multipath waveforms (caused by the Doppler effect) is caused by random displacements of the ith scatterer, as well as movements of the MS, i.e. $\mathbf{X}_i^S(t)$ and $\mathbf{v}t$, respectively. Apparently if time-variations are just caused by the scatterers' displacements, equation (6) transforms into the conventional linear Doppler caused by the straight motion (linear speed) of the MS [11]. Random displacements introduced in this paper are caused by different changes in the speed and/or the direction of movements of different scatterers, and have not been studied in a closed-form in the literature.

III. Effect of Scatterers' Random Displacements on the CCF

In this section we derive the STF-CCF between the CTFs of two arbitrary MIMO communication links $h_{pm}(t_1,\omega_1)$ and $h_{qn}(t_2,\omega_2)$, denoted by:

$$R_{pm;qn}(t_1,t_2;\omega_1,\omega_2) \triangleq E[h_{pm}(t_1,\omega_1)\ h_{qn}^*(t_2,\omega_2)], \quad (7)$$

1930-529X/07/$25.00 © 2007 IEEE

$$R_{pm;qn}(t_1,t_2;\omega_1,\omega_2) = \tag{8}$$
$$E\left[\sum_{i_1,i_2=1}^{I} G_p^B(\theta_{i_1}^B;\omega_1)G_m^M(\theta_{i_1}^M;\omega_1)g_{p,m;i_1}e^{-j\omega_1\tau_{p,m;i_1}(t_1)}e^{j(\phi_{i_1}-\phi_{i_2})}G_q^B(\theta_{i_2}^B;\omega_2)G_n^M(\theta_{i_2}^M;\omega_2)g_{q,n;i_2}e^{j\omega_2\tau_{q,n;i_2}(t_2)}\right].$$

$$R_{pm;qn}(t_1,t_2;\omega_1,\omega_2) = \frac{P}{I}\sum_{i_1,i_2=1}^{I}\left\{E\left[(\tau_{i_1}\tau_{i_2})^{\frac{-\eta}{2}}e^{j\left(\omega_2\tau_{i_2}-\omega_1\tau_{i_1}\right)}\right]E\left[G_p^B(\theta_{i_1}^B;\omega_1)G_q^B(\theta_{i_2}^B;\omega_2)e^{j\left(\frac{\omega_1}{c}\mathbf{a}_p^{B^T}\boldsymbol{\Theta}_{i_1}^B-\frac{\omega_2}{c}\mathbf{a}_q^{B^T}\boldsymbol{\Theta}_{i_2}^B\right)}\right]\right. \tag{9}$$
$$\left.\times E\left[e^{j(\phi_{i_1}-\phi_{i_2})}\right]E\left[G_m^M(\theta_{i_1}^M;\omega_1)G_n^M(\theta_{i_2}^M;\omega_2)e^{\frac{j}{c}\left(\omega_2\left(\mathbf{X}_{i_2}^S(t_2)+\mathbf{v}t_2-\mathbf{a}_n^M\right)^T\boldsymbol{\Theta}_{i_2}^M-\omega_1\left(\mathbf{X}_{i_1}^S(t_1)+\mathbf{v}t_1-\mathbf{a}_m^M\right)^T\boldsymbol{\Theta}_{i_1}^M\right)}\right]\right\}.$$

where (t_1,t_2) are sampling times, (ω_1,ω_2) are carrier frequencies and $(p,m;q,n)$ are antenna element indices. By replacing (6) in (7), we rewrite the CCF as follows: see (8). By re-grouping dependent and independent random variables in (8), using the approximation $g_{p,m;i}\approx g_i=\sqrt{\frac{P}{I}}\ {\tau_i}^{-\frac{\eta}{2}}$, and using Assumptions A1-A4, the expression of $R_{pm;qn}(t_1,t_2;\omega_1,\omega_2)$ is decomposed as follows: see (9). Based on Assumptions A4 and A8, the first expectation in (9) or $E\left[{\tau_i}^{-\eta}e^{j(\omega_2-\omega_1)\tau_i}\right]$ is calculated as $\boldsymbol{\Phi}_\tau^{(\eta)}\left(j(\omega_2-\omega_1)\right)$, where $\boldsymbol{\Phi}_\tau^{(\eta)}\triangleq E[\tau^{-\eta}e^{s\tau}]$ [8, Appendix I]. In order to calculate the last expectation in (9), we first perform the expectation on a simplified version of this expectation and for an arbitrary Wiener displacement process vector $\mathbf{X}(t)$ as follows:

$$E\left[e^{\frac{j}{c}(\omega_2\mathbf{X}(t_2)-\omega_1\mathbf{X}(t_1)+\mathbf{d})^T\boldsymbol{\Theta}_i^M}\right]= \tag{10}$$
$$E\left[E_{\mathbf{X}}\left[e^{\frac{j}{c}(\omega_2\mathbf{X}(t_2)-\omega_1\mathbf{X}(t_1))^T\boldsymbol{\Theta}_i^M}\right]e^{\frac{j}{c}\mathbf{d}^T\boldsymbol{\Theta}_i^M}\right],$$

where $E_{\mathbf{X}}[.]$ denotes the expectation with respect to the pdf of $\mathbf{X}$, $E[.]$ is the expectation with respect to the pdf of all remaining random variables, and $\mathbf{d}$ is an arbitrary 2D vector. After some manipulations and using the results of [11, Appendix I], two remaining expectations in (9) are calculated and led to the formulation of the CCF as follows:

$$R_{pm;qn}(t_1,t_2;\omega_1,\omega_2)=\frac{P}{I}\boldsymbol{\Phi}_\tau^{(\eta)}\left(j(\omega_2-\omega_1)\right)\times \tag{11a}$$
$$\mathcal{W}\left(\mathbf{d}_{p,q}^B,\mathcal{G}_{p,k}^B(\omega_1)\otimes{\mathcal{G}_{q,-k}^B}^*(\omega_2)\otimes\mathcal{F}_k^B\right)\times$$
$$\mathcal{W}\left(\mathbf{d}_{m,n}^M,\mathcal{G}_{m,k}^M(\omega_1)\otimes{\mathcal{G}_{n,-k}^M}^*(\omega_2)\otimes\mathcal{F}_k^M\right)\times$$
$$\left(\sum_{i=1}^{I}e^{-\zeta_i(t_2-t_1)\omega_2^2/2c^2}\times e^{-\zeta_i t_1(\omega_2-\omega_1)^2/2c^2}\right)$$

where $\boldsymbol{\Phi}_\tau^{(\eta)}(s)\triangleq E[\tau^{-\eta}e^{\tau}s]$ is the η-order integration of the MGF of the delay profile (DP),

$$\mathcal{W}(\mathbf{d},\mathcal{H}_k) \triangleq 2\pi\sum_{k=-\infty}^{+\infty}j^k e^{jk\angle\mathbf{d}}\mathcal{H}_k J_k(\frac{|\mathbf{d}|}{c}), \tag{11b}$$
$$\mathbf{d}_{p,q}^B \triangleq \omega_2\mathbf{a}_q^B-\omega_1\mathbf{a}_p^B, \tag{11c}$$
$$\mathbf{d}_{m,n}^M \triangleq (\omega_1t_1-\omega_2t_2)\,\mathbf{v}+\omega_2\mathbf{a}_n^M-\omega_1\mathbf{a}_m^M, \tag{11d}$$

$J_k(z)\triangleq\frac{j^{-k}}{\pi}\int_0^\pi e^{j(k\xi+z\cos\xi)}d\xi$ is the k^{th}-order Bessel function of the first kind, $|.|$ denotes Euclidian norm and $z_n\triangleq x_n\otimes y_n=\sum_{k=-\infty}^{+\infty}x_k y_{n-k}$ denotes the linear convolution of two given discrete-time sequences x_n and y_n.

Remark 1: As it is seen in (11a), the contribution of each moving scatterer is represented by its corresponding variance factor ζ_i; the more the variance factor is, the faster the ith associated term in the CCF decays. It implies that scatterers with larger displacements have less effect on the CCF, while the effect of slowly moving scatterers last longer.

IV. Effect of Scatterers' Random Displacements on the Power Spectral Density

In this section, we investigate how the scatterers' random movements affect the PSD of the channel process. This analysis is valid for the stationary case of $\omega_1=\omega_2=\omega$ and $m=n=1$. If the scatterers are fixed it can be shown that the PSD will be [11]:

$$\mathbf{R}_{p1,q1}(\Lambda,\omega)=\int_{-\infty}^{+\infty}e^{-j\Lambda\Delta t}R_{p1,q1}(t_1,t_2;\omega,\omega)d\Delta t$$
$$= \mathcal{W}(\mathbf{d}_{p,q}^B,\mathcal{H}_k^B)\frac{4\pi c}{\omega|\mathbf{v}|}P_0$$
$$\times \sum_{k=-\infty}^{+\infty}e^{jk\angle\mathbf{v}}(\mathcal{G}_{1,k}^M(\omega)\otimes\mathcal{G}_{1,-k}^M(\omega)\otimes\mathcal{F}_k^M)$$
$$\times \frac{T_k(\frac{c\Lambda}{|\mathbf{v}|\omega})}{\sqrt{1-(\frac{c\Lambda}{|\mathbf{v}|\omega})^2}},|\Lambda|<\frac{\omega}{c}|\mathbf{v}|, \tag{12}$$

where $\Delta t=t_2-t_1$. $\mathbf{R}^M(\Lambda)$ is defined as the last term in (12) which represents the impact of non-isotropic environment, the APP and the direction of the MS speed as follows:

$$\mathbf{R}^M(\Lambda)=\sum_{k=-\infty}^{+\infty}e^{jk\angle\mathbf{v}}(\mathcal{G}_{1,k}^M(\omega)\otimes\mathcal{G}_{1,-k}^M(\omega)\otimes\mathcal{F}_k^M)$$
$$\times \frac{T_k(\frac{c\Lambda}{|\mathbf{v}|\omega})}{\sqrt{1-(\frac{c\Lambda}{|\mathbf{v}|\omega})^2}},|\Lambda|<\frac{\omega}{c}|\mathbf{v}|, \tag{13}$$

where $T_k(\Lambda)$ is the k^{th} order Chebyshev polynomial function of the first kind. Please note that $\mathbf{R}^M(\Lambda)$ represents PSD of a bandlimited process. To consider the effect of scatterers'

1930-529X/07/$25.00 © 2007 IEEE

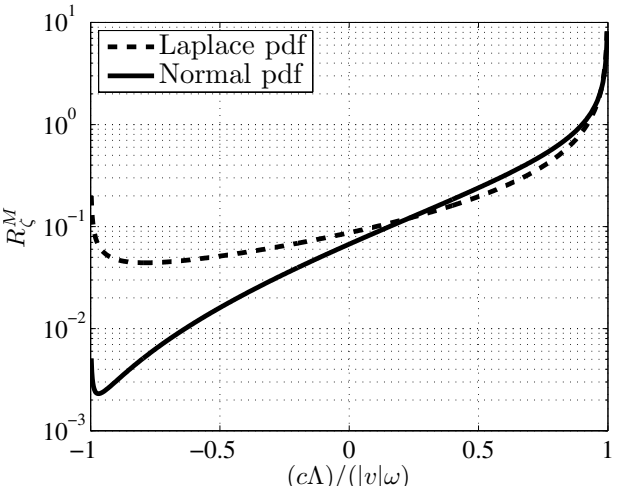

Fig. 2. PSD for the Laplace and Normal pdf case for fixed scatterers moving on the x-direction.

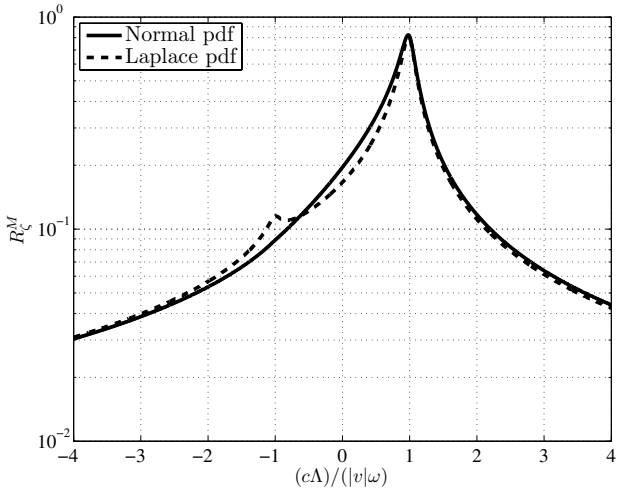

Fig. 3. PSD for the Laplace and Normal pdf case for moving scatterers moving on the x-direction.

random displacements on the channel PSD, it is easily noted that $\mathbf{R}^M(\Lambda)$ should be modified as in $\mathbf{R}_\zeta^M(\Lambda)$:

$$\mathbf{R}_\zeta^M(\Lambda) = \mathbf{R}^M(\Lambda) * \frac{1}{I}\sum_{i=1}^{I} \frac{1}{j\Lambda + \zeta_i\omega^2/2c^2}. \quad (14)$$

In figure 2 the PSD is depicted for a microcellular environment where omnidirectional antenna elements are used and the scatterers are fixed. To investigate the role of scatterers' movements, figure 3 depicts the same scenario with non-fixed scatterers ($I = 10$ and $\zeta_i = 0.05$).

It is clearly observed that the movement of scatterers has a great impact on the channel PSD, and causes the PSD to be a non-bandlimited process, in contrast to the fixed scatterers case.

V. Conclusions

Random movements of scatterers on the azimuth plane are characterized by two-dimensional independent-increment stationary-increment Wiener process vectors in terms of the amplitude and the direction of their speed. The effects of such movements are investigated on the CCF of a multi-path Rayleigh fading channel in terms of temporal, frequency, and spatial correlations. While the non-isotropic scattering and directional antennas introduce a linear combination of (first kind) Bessel functions with different orders to represent spatial-temporal-frequency selectivity aspects of the CCF, random displacements of the scatterers reshape the CCF in terms of available coherence bandwidth and coherence time. The results show that the realistic channel seen by a moving MS with constant speed and some scatterers with random displacements in the azimuth plane is far from what is believed in the conventional literature assuming fixed scatterers and moving MS. In fact random displacements of the scatterers (and maybe the MS) are subject to be incorporated in the resulting CCF. This work successfully takes into account the random displacements of scatterers (and the MS), while it also provides a solid platform to compute the CCF in an analytical form. It also considers the effect of these random movements on the channel process PSD.

References

[1] L. V. d. P. S. Thoen and M. Engels, "Modeling the channel time-variance for fixed wireless communications," *IEEE Communications Letters*, vol. 6, no. 8, pp. 331–333, 2002.

[2] A. F. Molisch, "A generic model for mimo wireless propagation channels," in *Proceedings of IEEE International Conference on Communications*, vol. 1, pp. 277–282, 2002.

[3] J. E. B. J. Medbo and F. Harrysson, "Temporal radio channel variations with stationary terminal," in *Vehicular Technology Conference, 2004. VTC2004-Fall. 2004 IEEE 60th*, vol. 1, pp. 91–95, 2004.

[4] "http://www.efunda.com/math/bessel/bessel.cfm."

[5] H. S. Rad and S. Gazor, "Effects of mobile station rotation on the correlation function of mimo wireless channels," *IEEE Transactions on Vehicular Technology*, September 2006. accepted with minor revisions.

[6] A. Papoulis and S. U. Pillai, *Probability, Random Variables, and Stochastic Processes*. McGraw-Hill, 4 ed., 2002.

[7] H. Stark and J. W. Wood, *Probability and Random Processes With Applications to Signal Processing*. Prentice Hall, 3 ed., 2002.

[8] S. Gazor and H. S. Rad, "Space-time-frequency characterization of mimo wireless channels," *IEEE Transactions on Wireless Communications*, vol. 5, pp. 2369–2375, September 2006.

[9] M. Kalkan and R. H. Clarke, "Prediction of the space-frequency correlation function for base station diversity reception," *IEEE Transactions on Vehicular Technology*, vol. 46, pp. 176–184, February 1997.

[10] H. Hashemi, "The indoor radio propagation channel," *Proceedings of the IEEE*, vol. 81, no. 7, pp. 943–968, 1993.

[11] H. S. Rad and S. Gazor, "The impact of non-isotropic scattering and directional antennas on mimo multicarrier mobile communication channels," *IEEE Transactions on Communications*, September 2006. accepted with minor revisions,.

[12] M. Stege, J. Jelitto, M. Bronzel, and G. Fettweis, "A multiple input - mutiple output channel model for simulation of tx and rx diversity wireless systems," in *52nd IEEE Conference on Vehicular Technology*, vol. 2, pp. 833–839, 2000.